A stochastic two-dimensional intelligent driver car-following model with vehicular dynamics

Hong-Sheng Qi(祁宏生)[1,†] and Yu-Yan Ying(应雨燕)[2]

[1] *College of Civil Engineering and Architecture, Zhejiang University, Hangzhou* 310058, *China*
[2] *College of Polytechnic, Zhejiang University, Hangzhou* 310015, *China*

(Received 20 July 2022; revised manuscript received 29 August 2022; accepted manuscript online 5 September 2022)

The law of vehicle movement has long been studied under the umbrella of microscopic traffic flow models, especially the car-following (CF) models. These models of the movement of vehicles serve as the backbone of traffic flow analysis, simulation, autonomous vehicle development, *etc*. Two-dimensional (2D) vehicular movement is basically stochastic and is the result of interactions between a driver's behavior and a vehicle's characteristics. Current microscopic models either neglect 2D noise, or overlook vehicle dynamics. The modeling capabilities, thus, are limited, so that stochastic lateral movement cannot be reproduced. The present research extends an intelligent driver model (IDM) by explicitly considering both vehicle dynamics and 2D noises to formulate a stochastic 2D IDM model, with vehicle dynamics based on the stochastic differential equation (SDE) theory. Control inputs from the vehicle include the steer rate and longitudinal acceleration, both of which are developed based on an idea from a traditional intelligent driver model. The stochastic stability condition is analyzed on the basis of Lyapunov theory. Numerical analysis is used to assess the two cases: (i) when a vehicle accelerates from a standstill and (ii) when a platoon of vehicles follow a leader with a stop-and-go speed profile, the formation of congestion and subsequent dispersion are simulated. The results show that the model can reproduce the stochastic 2D trajectories of the vehicle and the marginal distribution of lateral movement. The proposed model can be used in both a simulation platform and a behavioral analysis of a human driver in traffic flow.

Keywords: intelligent model, vehicular dynamics, stochastic differential equation, stochastic stability

PACS: 05.60.–k, 45.70.Vn **DOI:** 10.1088/1674-1056/ac8f3c

1. Introduction

1.1. Background

Microscopic vehicular modeling is a long-term research topic in traffic flow theory, and has received much attention in various fields, such as physics,[1] control theory,[2] and traffic engineering.[3] It connects microscopic behavior with the macroscopic traffic flow, such as the stop-and-go traffic phenomenon.[4] In the coming age of connected and autonomous vehicles (CAVs), the microscopic level model becomes even more important.[5] The CAV can obtain information about surrounding vehicles with high precision detectors, and a precise model of each driver-vehicle unit would benefit behavioral analysis, inference, and interactive predictions about human-driven vehicles.

One of the major microscopic level behaviors is car-following (CF). It depicts how a driver follows another car in the same lane. Major theoretical tools include the differential equation, and cellular model or CA for single-lane[6] or multi-lane,[7] lattice–gas model.[8] In differential types of CF models, a stimulus–reaction framework is established to map the system's state in response to the driver's reaction (including ego vehicle state and the state of surrounding vehicles). The stimuli are the states of surrounding vehicles (position, speed, acceleration, *etc.*), and an ego vehicle accelerating according to the states of surrounding vehicles. Major CF models[9] include the Gipps model, GM model, and intelligent driver model (IDM).[10] The IDM, which may be one of the most famous models, is used in major traffic flow simulation software. However, conventional CF models neglect the lateral movement,[11] which has proven unrealistic.[12–15] To overcome this drawback, two types of models, non-lane based[11] and 2D CF models,[13] are proposed. The former adds a lateral gap to the conventional CF model, and the latter explicitly considers the lateral movement. Although the above achievements provide significant insight into traffic flow evolution mechanism, two important aspects of the driver-vehicle unit dynamics , *i.e.*, 2D noise and the vehicle model, have not yet been considered. We used the generative process of vehicle trajectories (as shown in Fig. 1) to describe the necessity of the above two aspects in vehicle behavior modeling. A driver senses the traffic flow environment (such as the distance to a leading vehicle), decides on the best acceleration/steering, and then executes that decision (*i.e.*, to control the vehicle). Typically, a driver controls a vehicle by steering and accelerating and, if the vehicle deviates from the middle lane to the left, then the driver tends to steer right, and vice versa. By controlling the input, the vehicle moves and produces dynamic behavior. The end output of this process is real-time trajectory. In the microscopic traffic flow analysis, the trajectory is typi-

†Corresponding author. E-mail: qihongsheng@zju.edu.cn
© 2023 Chinese Physical Society and IOP Publishing Ltd

cally defined as being located at the middle point of the front bump. This process is influenced by many stochastic factors, including: (i) characteristics of the driver, such as age, driving level, emotional state; (ii) randomness of the road, and resulting road-vehicle interaction. For instance, the flatness of a road influences vehicle dynamics; (iii) the surrounding traffic flow dynamics is basically stochastic; (iv) environmental factors, such as rain and snow; (v) other stochastic factors, such as aging of the vehicle body. Traditional CF models can deal with partial elements of the above process (such as the stochastic acceleration). A full 2D stochastic microscopic model remains to be developed. To analyze the vehicle's final movement, vehicle dynamics and stochastic factors should be taken into account. Without the vehicle dynamics model, the generated trajectory may not be drivable and, without the stochastic consideration, the generated traffic flow dynamics may not be realistic. Currently, a model that considers the above two components remains to be developed, and such a development will make traffic flow simulation more realistic. Figure 2(b) shows the SUMO traffic flow simulation of vehicle dynamics and real world data. The vehicle trajectory almost does not fluctuate along the lane (3.7-m wide). The middle line of the lane is defined at $y = 1.85$ m. In Fig. 2(c), the real world high D dataset shows that even when keeping in a lane, the vehicles move in a stochastic way. This deviation reaches about 4m and its distribution is given in Fig. 2(a). For a single vehicle, the deviation in the trajectory is continuous. The driver constantly applies controls to the vehicle, so that the vehicle operates in an equilibrium way, both laterally and longitudinally. Current CF models mainly describe 1D movement (*i.e.*, longitudinal direction) by using the acceleration as input. Some extensions toward the 2D case are still lacking in vehicle dynamics and stochasticity considerations. As such, real world phenomena cannot be analyzed or reproduced by using those current models.

To remedy the above issues in this work, we combine the intelligent driver model framework, vehicle dynamics, and stochastic factors to formulate a stochastic 2D intelligent driver CF model with vehicle dynamics, based on the stochastic differential equation theory. The driver's control inputs include steering and acceleration, both of which are developed based on the idea of an intelligent driver model and an optimal velocity model. The 2D randomness is explicitly embedded since such considerations will make the model more realistic. Thus, compared with those current microscopic traffic models, the present model can reproduce realistic lateral stochastic movements that satisfy the physical constraint of the vehicle model.

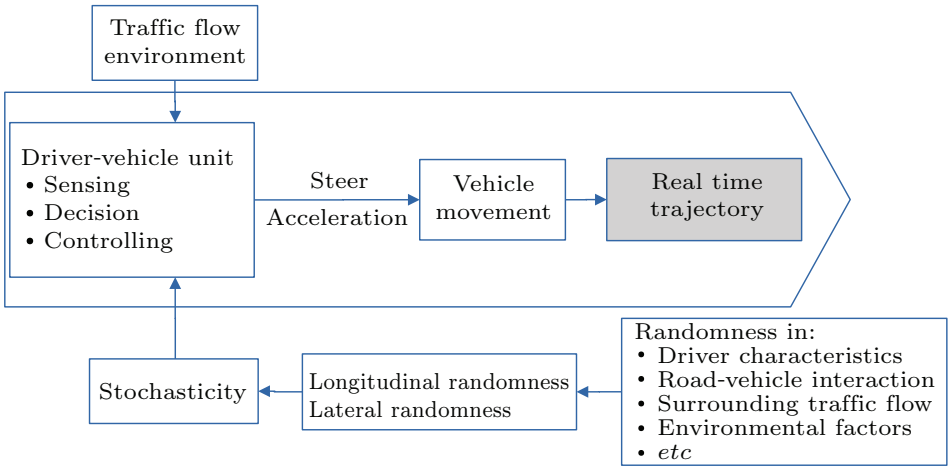


Fig. 1. Generation process of vehicular trajectories.

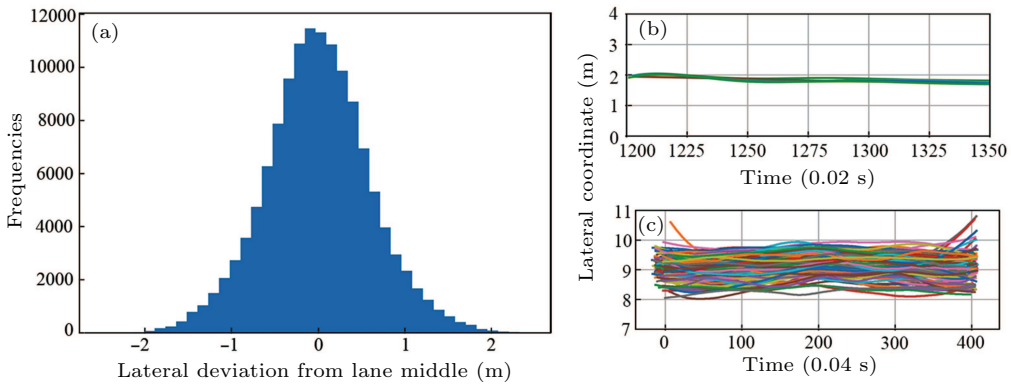


Fig. 2. Deviations of lane keeping trajectories in high D dataset, showing (a) lateral deviation distribution, (b) lateral evolution of simulation in SUMO, and (c) lateral evolution in high D dataset.

1.2. Literature review

1.2.1. CF model and its 2D extension

The CF model may-be is a most studied theoretical microscopic traffic flow behavior model. Typically, it is formulated by one or several ordinary differential equations. In the CF model, each vehicle is regarded as a single point, which is a reference point on the vehicle body. This reference point was typically defined as being located at the middle point of the front bumper.[16] Traditional CF was constructed on the basis of the stimulus–reaction framework (*i.e.*, the driver reacts to a change in the state of the leading vehicles, either in the current lane, or in a neighboring lane), by adjusting the ego vehicle's speed (or equivalent, through acceleration). Different models have been developed, based on different assumptions under this stimulus–reaction framework, including Pipes model,[17] GM model,[18] Gipps model,[19] and IDM model.[20] An appropriate microscopic traffic model should replicate the characteristics of macroscopic traffic flow.[21] For instance, the flow–density relationship, generated by the model, should be consistent with empirical observations.

The basic CF model only describes longitudinal dimension movement, while the lateral counterpart is totally neglected. On the other hand, with the development of CAV technology, the demand for detailed 2D vehicular modeling is increasing. To deal with this issue, the basic CF framework is extended toward a 2D model, or is enhanced with weak-lane discipline. The former one equips the traditional CF model with lateral dimensional dynamics (lateral acceleration or speed), while the latter counterpart mainly refers to the non-lane based model, with weak lane discipline. Regarding the former type, Delpiano *et al.*[22] proposed a 2D car model that considers the lateral friction effect. Sharath and Velaga[13] extended the 1D IDM model to a 2D case. The effective lateral gap is defined. Basically, the input–output structure is the same as that of IDM model: the outputs of the model are accelerations, although the lateral and longitudinal components are decomposed. For the weak-lane-based models, the common CF framework is also inherited. The lateral gap was defined in Ref. [23]. These models partly solve the problems of traditional CF models. However, vehicular dynamics were not considered in these models. The reference point of the model is defined to be located at the middle point in the front bumper. Thus, the results from the model may be unsuitable for the vehicle because the vehicle has a certain physical size and its movement is implemented by manipulating steering and acceleration s. Besides, the stochasticity is still not embodied very well in the model framework. The simulation platform, such as SUMO or Carla, cannot replicate traffic-flow characteristics, as shown in Fig. 2(b). It is concluded that to better understand traffic phenomena, a microscopic traffic-flow model, with vehicle dynamics and stochasticity embodied, is necessary.

1.2.2. Stochastic microscopic traffic-flow model

It is obvious that the road traffic flow is stochastic[24] and major cars that follow models are developed as a deterministic system. However, some macroscopic level phenomena are closely related to stochasticity,[25] such as oscillation,[10] packet loss,[26] and instability.[27,28] Some researchers extended traditional models with a different randomness consideration. These extensions included white acceleration noise,[10] Brownian motion,[29,30] geometric Brownian motion,[31] and OU process.[14] The basis models may be either simple models with different regimes or complex IDM models. With these stochasticity considerations, some phenomena, including speed–density relationship and oscillation can be explained or reproduced. However, it should be noted that noise exits at both lateral dimension and longitudinal dimension, while a majority of the stochastic models focused on a single dimension noise. On the other hand, just like the traditional microscopic traffic-flow model, a vehicle is represented by a single point, which neglects vehicular model and control input, such as a driver's steering manipulations.

1.3. Objectives, manuscripts, and contributions

It can be seen that the current microscopic traffic-flow behavior model either neglects the vehicle dynamics factor, or overlooks 2D noise. To fill this gap, we consider the following three components simultaneously: 2D noise, vehicle model with acceleration and steering input, and intelligent driver idea. The 2D movement is then formulated as a stochastic differential equation system. Contributions include the following points.

(I) A 2D driver-vehicle unit model is constructed that explicitly considers 2D noise.

(II) Control inputs include steering and acceleration, and both are constructed from the ideas in a conventional IDM model and an optimal velocity model.

(III) Stochastic stability is analyzed by using the Lyapunov method.

The remainder of this paper is organized as follows. The model is presented in Section 2, and the stochastic stability condition is analyzed in Section 3. In Section 4, the behavior of the model is examined by using numerical simulation method. The last section is devoted to the remarks concerning future model development and applications.

2. Model development

2.1. Notations

Symbols are given below in the following descriptions.

$l_{\rm f}(l_{\rm r}), l_{\rm F}(l_{\rm R})$ are the distance of front (rear) wheel and front (rear) bumper to the CG.

$[x_i, y_i, \psi_i]$ is the vehicle state vector for vehicle i. x and y are coordinates of CG, and ψ is heading angle.

$\psi_i^{\rm E}$ is the desired (or expected) heading angle of vehicle i; δ_i^* is the desired steering rate of vehicle i.

$[a_i, \gamma_i]^{\rm T}$ is the control input of vehicle i, speed and steering rate of front wheel.

$Q = [q_1, q_2, q_3, q_4, q_5, q_6, q_7] = [x, y, \psi, v, \delta, z_{\rm lat}, z_{\rm long}]$, Q is the extended state vector of one vehicle. $z_{\rm lat}$ and $z_{\rm long}$ each are 2D noise.

$\mathrm{d}Q = F(Q)\,\mathrm{d}t + L(Q)\,\mathrm{d}W$, F and L are drift and diffusion terms. $F = [f_1, f_2, \ldots, f_7]^{\rm T}$ and $L = [l_1, l_2, \ldots, l_7]^{\rm T}$.

θ, μ, and σ are parameters of Ornstein–Uhlenbeck process.

$\Gamma_{\rm acc}$ and $\Gamma_{\rm steer}$ are functions that map the control input to a reasonable interval.

K and $Z_{\rm bnd}$ are meta noise and bounded noise.

$\sigma_{\rm lon}$ and $\sigma_{\rm lat}$ are noise level of two dimensions.

$Z_{\rm lat}$ and $Z_{\rm long}$ are 2D tire noise.

$\eta_{\rm long}$ and $\eta_{\rm lat}$ are sensitivities to 2D noise of the system state.

s_i is the gap between vehicles i and its leading vehicle $i-1$. s_i^* is the desired gap. s_0 is the minimum gap.

$a_{\rm MAX}$ is the maximal acceleration, b is the comfortable deceleration of follower, T is safe time headway, $v_{\rm d}$ is the desired speed.

τ is the parameter in $\mathrm{IDM}_{\rm steering}$.

$\mathrm{IDM}_{\rm acc}$ and $\mathrm{IDM}_{\rm steer}$ are shortcuts of functions that calculate acceleration and steering rate by using an idea borrowed from IDM model.

$O(\delta_i^*)$ is the optimal steering angle. δ_i^* is the desired steering angle.

$\Delta\xi_1$ and $\Delta\xi_2$ are angle difference between current position and desired position.

$V(Q)$ and $LV(Q)$ are Lyapunov function and drift term of the V respectively.

Δt is the time step for simulation and ΔW is the bivariate Gaussian variable.

2.2. Model framework

The basic setting of the model is given in Fig. 3. In Fig. 3(a), a single track model is used to illustrate a description of vehicle dynamics, while in Fig. 3(b), there are a leader vehicle and a follower vehicle within the lane. Traditional models assume that the two are located exactly in the middle line, with a heading angle of zero (*i.e.* points are exactly in the longitudinal direction). In our model framework, the vehicles move freely in the x–y plane, under physical constraints (such as maximal steering angle). Given the above basic setting, the model framework is given in Fig. 3(c). We use a single track model (in Fig. 3(a)) as a default vehicular dynamics model. Our framework can accommodate other vehicular models. Control input of the single track model includes the steering rate and the acceleration, with both being modeled by using ideas borrowed from the IDM and optimal velocity models. The 2D randomness is taken into account by the Brownian motion in Subsubsection 2.3.3. These considerations finally lead to the stochastic 2D IDM model with vehicular dynamics in Subsection 2.4. Figure 3(c) also denotes the corresponding sections where the model development is located.

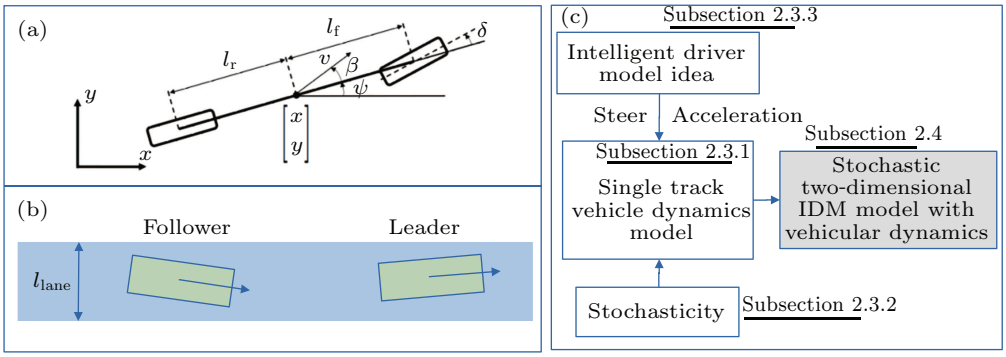


Fig. 3. Basic setting: (a) definition of state of typical vehicle; (b) modeling scenario, and (c) manuscript organization.

2.3. Model components

2.3.1. Basic vehicular dynamics model

There are many vehicle models available, from a point mass model[32] to a multi-body vehicle dynamics model.[33] These models differ in the abstraction level. This research mainly focuses on the enhancement of the conventional CF model with lateral dynamics. Thus, a vehicle model with acceleration and steering control input is appropriate. The Rajamani vehicle model[34] is employed here. More complex vehicle models may lead to analytical burdens or undesired complexity.[35] For the Rajamani model, a vehicle's physical configuration is given in Fig. 4. The coordinate of the vehicle is given by the location of center of gravity (CG), *i.e.* (x_i, y_i). The distance from the CG to the front bumper and the rear bumper are given by $l_{\rm F}$ and $l_{\rm R}$, respectively, while the distance

from the CG to the front axle and the rear axle are denoted by $l_{\rm f}$ and $l_{\rm r}$, respectively. Its heading angle is ψ_i. For simplicity, so no confusion, we will sometimes omit the vehicle index j or time dimension, *i.e.*, we adopt $x(t)$, $y(t)$, and $\psi(t)$ or x_i, y_i, and ψ_i. Therefore, the state of the vehicle is given by the vector $[x, y, \psi]$. The original control input is the front wheel steering angle δ and speed v. They will be formulated later by using an idea borrowed from the IDM model. The Rajamani model is given in Eq. (1).

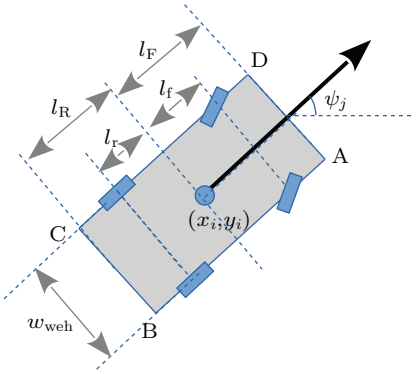


Fig. 4. Vehicle illustration.

$$\dot{x} = v\cos(\psi+\beta), \tag{1a}$$

$$\dot{y} = v\sin(\psi+\beta), \tag{1b}$$

$$\dot{\psi} = \frac{v\cos(\beta)\tan\left(\delta^f\right)}{l_{\rm f}+l_r}. \tag{1c}$$

The β in Eq. (1) is given by

$$\beta = \tan^{-1}\left(\frac{l_{\rm r}\tan\delta^f}{l_{\rm f}+l_{\rm r}}\right). \tag{2}$$

The above model uses speed and the steering angle as control input. The difference between the two control inputs lie in the acceleration $a_{\rm long}$ and the steering rate v_δ. We can further use the two variables as control input to the model. The model in Eq. (1) is formulated as follows:

$$\dot{x} = v\cdot\cos\left(\psi+\tan^{-1}\left(\frac{l_{\rm r}\tan\delta}{l_{\rm f}+l_{\rm r}}\right)\right), \tag{3a}$$

$$\dot{y} = v\cdot\sin(\psi+\tan^{-1}\left(\frac{l_{\rm r}\tan\delta}{l_{\rm f}+l_{\rm r}}\right)), \tag{3b}$$

$$\dot{\psi} = \frac{v\cdot\cos\left(\tan^{-1}\left(\frac{l_{\rm r}\tan\delta}{l_{\rm f}+l_{\rm r}}\right)\right)\tan(\delta)}{l_{\rm f}+l_{\rm r}}, \tag{3c}$$

$$\dot{v} = a_{\rm long}, \tag{3d}$$

$$\dot{\delta} = v_\delta. \tag{3e}$$

The control input of the vehicle includes the steering rate (*i.e.*, $v_\delta \overset{\rm def}{=} \dot{\delta}$) and the longitudinal acceleration $a_{\rm long}$. The control input and state variable are bounded. The constraint of the steering angle, speed, acceleration, and steering rate are bounded from both sides:

$$\delta\in\left[\underline{\delta},\overline{\delta}\right],\ v\in[\underline{v},\overline{v}],\ a_{\rm long}\in[\underline{a},\overline{a}],\ v_\delta\in\left[\underline{v_\delta},\ \overline{v}_\delta\right]. \tag{4}$$

The final acceleration input a should satisfy the above maneuver limits, and is formulated as follows:

$$\begin{aligned} a &= \Gamma_{\rm acc}\left(v, a_{\rm long}\right) \\ &= \begin{cases} 0, & \text{for } \left(v\le\underline{v}\wedge a_{\rm long}\le 0\right) \\ & \quad \bigvee\left(v\ge\overline{v}\wedge a_{\rm long}\ge 0\right)(C2), \\ \underline{a}, & \text{for } C2\wedge a_{\rm long}\le\underline{a}, \\ \overline{a}(v), & \text{for } C2\wedge a_{\rm long}\ge\overline{a}(v), \\ a_{\rm long}, & \text{otherwise.} \end{cases} \end{aligned} \tag{5}$$

Similarly, the steering rate γ is formulated as follows, with the maneuver limit considered:

$$\begin{aligned} \gamma &= \Gamma_{\rm steer}\left(\delta, v_\delta\right) \\ &= \begin{cases} 0, & \text{for } \left(\delta\le\underline{\delta}\wedge v_\delta\le 0\right) \\ & \quad \bigvee\left(\delta\ge\overline{\delta}\wedge v_\delta\ge 0\right)(C1), \\ \underline{v_\delta}, & \text{for } \neg C1\wedge v_\delta\le\underline{v_\delta}, \\ \overline{v}_\delta, & \text{for } \neg C1\wedge v_\delta\ge\overline{v}_\delta, \\ v_\delta, & \text{otherwise.} \end{cases} \end{aligned} \tag{6}$$

2.3.2. Driver behavior modeling

The driver manipulates the vehicle by steering and acceleration, so that the vehicle is centered within a lane and, at the same time, a suitable gap from leading vehicle is maintained. Owing to stochasticity, the vehicle is disturbed continuously from its equilibrium, and control input should be constantly implemented. We assume that the theoretical structures for the two control inputs (steering rate γ and acceleration a) are similar to each other. For acceleration, we revise the conventional IDM model to accommodate the 2D case; for steering, we borrow an idea from the optimal velocity model, and formulate the steering rate. The two behaviors will be invesigated later.

(i) Control input of the acceleration

For the acceleration control input, we use the traditional form of IDM, but with some revisions so that it can adapt to the 2D case. The conventional formulation of IDM is as follows:[36]

$$\begin{aligned} a_i &= a_{\rm MAX}\left[1-\left(\frac{v}{v_d}\right)^4-\left(\frac{s^*}{s_i}\right)^2\right], \\ s^* &= s_0+vT+\frac{v\Delta v}{2\sqrt{ab}}. \end{aligned} \tag{7}$$

Suppose that $l_{\rm F}+l_{\rm R}$ is the length of a vehicle. Without loss of generality, we assume that the vehicles have all this same length, but this length can be easily adjusted. We define the gap (*i.e.*, s_i) and the relative speed in a 2D case as follows:

$$\begin{aligned} s &= \sqrt{(x_i-x_{i-1})^2+(y_i-y_{i-1})^2}-(l_{\rm F}+l_{\rm R}), \\ \Delta v &= v_i-v_{i-1}. \end{aligned} \tag{8}$$

Equation (8) is basically the extension of a gap to the 2D case. We replace the gap and the relative speed in the original IDM model and, then, we have a new formulation of acceleration in a 2D case:

$$a = a_{\mathrm{MAX}}\left[1-\left(\frac{v}{v_d}\right)^4-\left(\frac{s_0+v_iT+\frac{v_i(v_i-v_{i-1})}{2\sqrt{a_{\mathrm{MAX}}b}}}{\sqrt{(x_i-x_{i-1})^2+(y_i-y_{i-1})^2}-(l_{\mathrm{F}}+l_{\mathrm{R}})}\right)^2\right] \stackrel{\mathrm{def}}{=} \mathrm{IDM}_{\mathrm{acc}}(x_i,y_i,v_i), \tag{9}$$

where $\mathrm{IDM}_{\mathrm{acc}}(\cdot,\cdot,\cdot)$ is shorthand for the function for calculating the acceleration input.

(ii) Control input of steering

The basic role of steering control is to center a vehicle within a lane and to make sure that the vehicle will not deviate too much from the middle line of that lane. Once the vehicle is located on the left of a middle line, then that vehicle should steer to the right, or *vice versa*. Following the stimulus–reaction analysis framework, we assume that there are two basic stimuli for the steering maneuver, which are illustrated in Fig. 5. We assume that there is an ideal (or target) location for the vehicle (target position in Fig. 5). Such a target position is the equilibrium state, if the speed of the leading vehicle (leader in Fig. 5) remains unchanged. The speed of the leader vehicle is indicated by v_{i-1}. The equilibrium headway is given by

$$s^{\mathrm{equi}} = (s_0+v_{i-1}T)\left(1-\frac{v_{i-1}}{v_d}\right)^{-1/2}. \tag{10}$$

The target position can be calculated to be $x_{i-1}+s^{\mathrm{equi}}$, thus

$$x_i^{\mathrm{d}} = x_{i-1}+(s_0+v_{i-1}T)\left(1-\frac{v_{i-1}}{v_d}\right)^{-1/2}. \tag{11}$$

The heading angle of the target position is ψ_i^{E} for vehicle i. Here, superscript 'E' indicates the expectation. In our case where the middle line of the lane overlaps the x-axis, ψ_i^{E} is zero exactly. Two stimuli ($\Delta\xi_1$ and $\Delta\xi_2$ in Fig. 5) exist for the steering manipulation of the driver. i) Under ideal conditions, ψ_i will converge to ψ_i^{E} by the steering operation, and the difference between the two is the first stimulus; ii) there is a certain difference in angle between the expected heading angle and the angle between the lines connecting the CGs of the two positions (*i.e.*, current position and target position). The line should overlap the middle line of the lane. The difference between the two angles is regarded as the second stimulus. If any of the above two stimuli deviates from ideal conditions, the driver has motivation to steer the vehicle to the left or to the right. The definitions of $\Delta\xi_1$ and $\Delta\xi_2$ are as follows:

$$\Delta\xi_1 = \psi_i^{\mathrm{E}}-\psi_i, \tag{12a}$$

$$\Delta\xi_2 = \psi_i^{\mathrm{E}}-a\cos\left(\frac{x_i-x_i^{\mathrm{d}}}{\sqrt{\left(x_i-x_i^{\mathrm{d}}\right)^2+\left(y_i-y_i^{\mathrm{d}}\right)^2}}\right). \tag{12b}$$

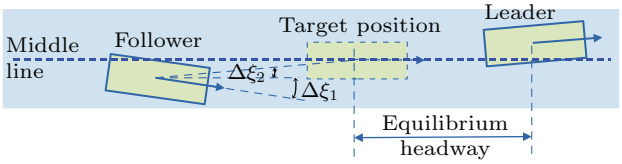


Fig. 5. Intelligent steering model.

Equation (12a) is the heading angle difference, and equation (12b) is basically the difference between the lane's middle line and the line connecting the CGs of the two positions. When $\Delta\xi_1=0$ and $\Delta\xi_2=0$, the driver has no incentive to manipulate steering. Therefore, we define the ideal steering angle as follows:

$$\delta_i^* = 1-\exp\left(\frac{\Delta\xi_1+\Delta\xi_2}{\tau}\right), \tag{13}$$

where τ is a parameter. We borrow the idea from the optimal velocity model,[8] and define the steering rate γ_i as follows:

$$\gamma_i = O(\delta_i^*)-\delta_i \stackrel{\mathrm{def}}{=} \mathrm{IDM}_{\mathrm{steer}}(x_i,y_i,\psi_i,\delta_i). \tag{14}$$

The function $O(\delta_i^*)$ is constructed as $O(\delta_i^*)=\tanh(\delta_i^*)$, as given by Bando *et al.*,[8] but with a slight revision made here. The original formulation is $\tanh(\delta_i^*-2)-\tanh(2)$. This formulation will make the steering manipulation asymmetric (steering to the left or right should be symmetrical around the lane's middle line). Finally, we have the steering rate formulation as follows:

$$\gamma_i = \mathrm{IDM}_{\mathrm{steer}}(x_i,y_i,\psi_i,\delta_i) = \tanh\left(1-\exp\left[\frac{2\psi_i^{\mathrm{E}}-\psi_i-a\cos\left(\frac{x_i-x_i^{\mathrm{d}}}{\sqrt{\left(x_i-x_i^{\mathrm{d}}\right)^2+\left(y_i-y_i^{\mathrm{d}}\right)^2}}\right)}{\tau}\right]\right). \tag{15}$$

2.3.3. Stochastic noise

We suppose that noises exist in both dimensions. Stochasticity may come from road-vehicle interaction, air drag, or others. Following Eq. (13) we use the Ornstein–Uhlenbeck (OU process, or Vasicek model in financial modeling) to model the noise. The OU process has the following attributes: (i) it fluctuates around an equilibrium value (which can be used

to mimic different expectation values of noise in traffic flow) and (ii) unlike the Brownian motion, it has finite variance (the noise variance in traffic flow should be finite). The OU process Z is expressed as

$$\mathrm{d}Z = \theta\left(\mu - Z\right)\mathrm{d}t + \sigma\,\mathrm{d}W. \tag{16}$$

The parameters of the above OU process have clear physical meanings: θ, which is a positive number, is the speed of reversion; μ is the long-run equilibrium value of the process, and σ is explained as the volatility. We want the equilibrium state of the process to be zero (the driver will finally center the vehicle within the lane) and, as such, we set μ to zero. Then, the OU process becomes $\mathrm{d}Z = -\theta Z\mathrm{d}t + \sigma\mathrm{d}W$. The resulting Z will fluctuate around 0. The sample paths are given with different parameters in the following figure, showing that the parameters can be adjusted to accommodate different levels of noise.

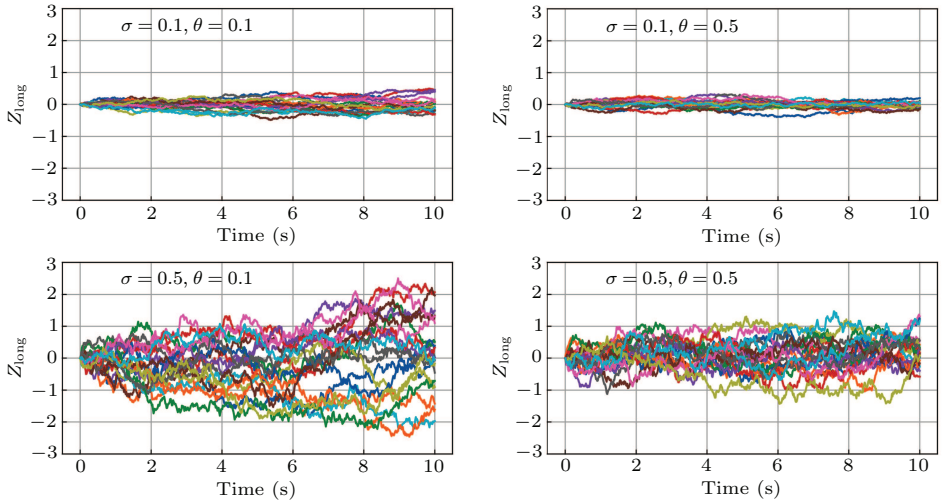


Fig. 6. Simulation paths of the noise with different parameter settings.

However, since the noise in the driving process is bounded, we need to transform the above OU noise to a certain extent and then embed the transformed noise into the system model. We use the hyperbolic tangent function to convert the OU process and, then, add the noise to the control input. The 2D noise is formulated by using the OU process as follows:

$$\begin{aligned}\mathrm{d}Z_{\mathrm{long}} &= -\theta_{\mathrm{long}}Z_{\mathrm{long}}\,\mathrm{d}t + \sigma_{\mathrm{long}}\,\mathrm{d}W,\\ \mathrm{d}Z_{\mathrm{lat}} &= -\theta_{\mathrm{lat}}Z_{\mathrm{lat}}\,\mathrm{d}t + \sigma_{\mathrm{lat}}\,\mathrm{d}W.\end{aligned} \tag{17}$$

Now, we embed the noise into the vehicular dynamics model in Eq. (3). We use the symbols η_{lat} and η_{long} to indicate sensitivity to the noise. As the acceleration represents the longitudinal maneuver and the steering mainly represents a lateral adjustment, we embed the noise in the model as follows:

$$\begin{aligned}\mathrm{d}v_i &= \Gamma_{\mathrm{acc}}\left(\mathrm{IDM}_{\mathrm{acc}}\left(x_i,y_i,v_i\right) + \eta_{\mathrm{long}}\tanh\left(Z_{\mathrm{long}}\right)\right)\mathrm{d}t,\\ \mathrm{d}\delta_i &= \Gamma_{\mathrm{steer}}\big(\mathrm{IDM}_{\mathrm{steer}}\left(x_i,y_i,\psi_i,\delta_i\right)\\ &\quad + \eta_{\mathrm{lat}}\tanh\left(Z_{\mathrm{lat}}\right)\big)\,\mathrm{d}t.\end{aligned} \tag{18}$$

2.4. Stochastic 2D intelligent driver model with vehicle dynamics

Combine the vehicles dynamics model, the 2D noise, and the IDM logic of steering and acceleration, then we will finally obtain a formulation for a stochastic 2D IDM model of vehicle I, with formula of vehicle dynamicsare as follows:

$$\begin{aligned}\mathrm{d}x_i &= \left[v_i\cdot\cos\left(\psi_i + \mathrm{atan}\left(\frac{l_{\mathrm{r}}\tan\delta_i}{l_{\mathrm{f}}+l_{\mathrm{r}}}\right)\right)\right]\mathrm{d}t,\\ \mathrm{d}y_i &= \left[v_i\cdot\sin\left(\psi_i + \mathrm{atan}\left(\frac{l_{\mathrm{r}}\tan\delta_i}{l_{\mathrm{f}}+l_{\mathrm{r}}}\right)\right)\right]\mathrm{d}t,\\ \mathrm{d}\psi_i &= \left[\frac{v_i\cdot\cos\left(\mathrm{atan}\left(\frac{l_{\mathrm{r}}\tan\delta_i}{l_{\mathrm{f}}+l_{\mathrm{r}}}\right)\right)\tan\left(\delta_i\right)}{l_{\mathrm{f}}+l_{\mathrm{r}}}\right]\mathrm{d}t,\\ \mathrm{d}v_i &= \Gamma_{\mathrm{acc}}\left(\mathrm{IDM}_{\mathrm{acc}}\left(x_i,y_i,v_i\right) + \eta_{\mathrm{long}}\tanh\left(Z_{\mathrm{long}}\right)\right)\mathrm{d}t,\\ \mathrm{d}\delta_i &= \Gamma_{\mathrm{steer}}\big(\mathrm{IDM}_{\mathrm{steer}}\left(x_i,y_i,\psi_i,\delta_i\right) + \eta_{\mathrm{lat}}\tanh\left(Z_{\mathrm{lat}}\right)\big)\,\mathrm{d}t,\\ \mathrm{d}Z_{\mathrm{long}} &= -\theta_{\mathrm{long}}Z_{\mathrm{long}}\,\mathrm{d}t + \sigma_{\mathrm{long}}\,\mathrm{d}W,\\ \mathrm{d}Z_{\mathrm{lat}} &= -\theta_{\mathrm{lat}}Z_{\mathrm{lat}}\,\mathrm{d}t + \sigma_{\mathrm{lat}}\,\mathrm{d}W.\end{aligned} \tag{19}$$

The undetermined parameters (except the parameters in the IDM model, which can be borrowed from existing research) include θ_{long}, θ_{lat}, σ_{long}, σ_{lat}, η_{long}, and η_{lat}. We formulate the above complex equation as a matrix form as follows:

$$\mathrm{d}Q = F\left(Q\right)\mathrm{d}t + L\left(Q\right)\mathrm{d}W = \begin{bmatrix} f_1 \\ \cdots \\ f_7 \end{bmatrix}\mathrm{d}t + \begin{bmatrix} l_1 \\ \cdots \\ l_7 \end{bmatrix}\mathrm{d}W. \tag{20}$$

The functions of f_1–f_7, and l_1–l_7 are obvious from Eq. (19). In the numerical section, we needed a discretization scheme to simulate the system dynamics. Here, we use the Euler discretization scheme for SDE as follows:

$$Q\left(k+1\right) = Q\left(k\right) + F\left(Q\left(k\right)\right)\Delta t + L\left(Q\left(k\right)\right)\Delta W, \tag{21}$$

where Δt is the time step duration, ΔW is a 2D Gaussian variable with zero mean. The two dimensions refer to longitudinal

direction and lateral direction . The covariance matrix is given by $\begin{bmatrix} \Delta t & 0 \\ 0 & \Delta t \end{bmatrix}$. Given an initial state $Q(0)$, the system evolution can be simulated.

3. Stochastic Lyapunov stability analysis

The system *i.e.*, equation (19) describes the 2D movement of the vehicle and is an SDE driven by the Brownian motion. We, then, analyze the stability of the SDE. Unlike a deterministic ODE, the stability of an SDE is explained from a probabilistic view point. First, we analyze the equilibrium point by assuming that a leader vehicle (labeled as $i-1$) is driving at a constant speed v_{i-1}. Under equilibrium conditions, the speed of the follower vehicle, *i.e.*, vehicle i is also v_{i-1}, and the acceleration rate and steering rate are both zero. The heading angles ψ_i and y_i should be zero also. Assuming that the leading vehicle travels at a constant speed, the equilibrium points are expressed as

$$Q^{\mathrm{EQU}} = [v_{i-1}t,\ 0,\ 0,\ 0,\ 0,\ 0,\ 0]^{\mathrm{T}}. \tag{22}$$

We denote error vector as $M = Q - Q^{\mathrm{EQU}} \overset{\mathrm{def}}{=} [m_1, m_2, \ldots, m_7]$. As Q is a stochastic process that is described by Eq. (19), the M is a stochastic process also. Clearly, each component of M is differentiable two times. Hence, according to the Ito formula, we have the formulation of M as shown in equations (23). The derivation is common and, thus, we omit the process. Note that Eq. (23b)–(23e) can be directly inherited from Eq. (19), as the function component in M is just the variable itself. The major difference between Eq. (19) and Eq. (23) lies in Eq. (23a).

$$\begin{aligned} \mathrm{d}m_1 = &\left[-v_{i-1} + (m_4 - v_{i-1}) \right. \\ &\left. \cdot \cos\left(m_3 + \operatorname{atan}\left(\frac{l_{\mathrm{r}} \tan m_5}{l_{\mathrm{f}} + l_{\mathrm{r}}} \right) \right) \right] \mathrm{d}t, \end{aligned} \tag{23a}$$

$$\mathrm{d}m_2 = \left[(m_4 - v_{i-1}) \cdot \sin\left(m_3 + \operatorname{atan}\left(\frac{l_{\mathrm{r}} \tan m_5}{l_{\mathrm{f}} + l_{\mathrm{r}}} \right) \right) \right] \mathrm{d}t, \tag{23b}$$

$$\mathrm{d}m_3 = \left[\frac{(m_4 - v_{i-1}) \cdot \cos\left(\operatorname{atan}\left(\frac{l_{\mathrm{r}} \tan m_5}{l_{\mathrm{f}} + l_{\mathrm{r}}} \right) \right) \tan(m_5)}{l_{\mathrm{f}} + l_{\mathrm{r}}} \right] \mathrm{d}t, \tag{23c}$$

$$\mathrm{d}m_4 = \Gamma_{\mathrm{acc}} \left(\mathrm{IDM}_{\mathrm{acc}}(m_1, m_2, m_4) + \eta_{\mathrm{long}} \tanh(m_6) \right) \mathrm{d}t, \tag{23d}$$

$$\begin{aligned} \mathrm{d}m_5 = &\Gamma_{\mathrm{steer}} \left(\mathrm{IDM}_{\mathrm{steer}}(m_1, m_2, m_3, m_5) \right. \\ &\left. + \eta_{\mathrm{lat}} \tanh(m_7) \right) \mathrm{d}t, \end{aligned} \tag{23e}$$

$$\mathrm{d}m_6 = -\theta_{\mathrm{long}} m_6 \, \mathrm{d}t + \sigma_{\mathrm{long}} \, \mathrm{d}W, \tag{23f}$$

$$\mathrm{d}m_7 = -\theta_{\mathrm{lat}} m_7 \, \mathrm{d}t + \sigma_{\mathrm{lat}} \, \mathrm{d}W. \tag{23g}$$

We express Eq. (23) by using matrix form $\mathrm{d}M = \mathcal{F}(M)\,\mathrm{d}t + \mathcal{L}(M)\,\mathrm{d}W$. $\mathcal{F}$ and $\mathcal{L}$ should be clear from the context. With the above formulation, the stochastic stability can be defined as follows.

Definition 1 stochastic stability. The system is stochastically stable if there exists $\delta = \delta(r, \xi) > 0$, for any $r > 0$ and $\xi > 0$ so that for any initial condition $M(0) \in S_\delta$ (where $S_\delta = \{|M| < \delta\}$), the following condition holds:

$$p\{\omega : |M(t)| < \delta \forall t \geq 0\} > 1 - \xi. \tag{24}$$

To analyze the stability, we construct the Lyapunov function $V(M)$ as follows:

$$V(M) = \frac{\sum_i (m_i)^2}{2}. \tag{25}$$

The scale factor $1/2$ is just for simplifying derivation. The first order differential V_M and the second order differential V_{MM} of the function $V(M)$ are

$$V_M = (m_i)^{\mathrm{T}} \quad \text{and} \quad V_{MM} = E, \tag{26}$$

where E is the identity matrix. As M is a stochastic process as described by Eq. (23), Lyapunov function V is also a stochastic process, which can be derived based on Ito theorem and given by

$$\mathrm{d}V = LV(M)\,\mathrm{d}t + V_M(M) \cdot \mathcal{L}(M)\,\mathrm{d}W. \tag{27}$$

In the above equation

$$\begin{aligned} LV(M) &= V_t + V_M \mathcal{F} + \frac{1}{2} \mathrm{trace}\left(\mathcal{L}^{\mathrm{T}} V_{MM} \mathcal{L} \right) \\ &= \frac{1}{2} \sum_i \mathcal{L}_i^2 + \sum_i m_i \mathcal{F}_i. \end{aligned} \tag{28}$$

Using the Lyapunov function and $LV(M)$, the stability condition can be specified as follows. Let $\mathcal{K}$ denote the family of all continuous non-decreasing functions $\mu : R_+ \to R_+$ such that $\mu(0) = 0$ and $\mu(r) > 0$ if $r > 0$; and $\mathcal{K}_\infty$ denotes the family of all functions $\mu \in \mathcal{K}$ such that $\mu(r) = \infty$. For $h > 0$, let $S_h = \left\{ M \in R^7 : |M| < h \right\}$. Then, according to Ref. [37], if there exist a Lyapunov function V and $\mu \in K$ such that $V(0,t) = 0$, then $\mu(|M|) \leq V(Mt)$ and $LV(M,t) \leq 0$ for all $(M,t) \in S_h \times R_+$. Therefore, the solution of the SDE is stochastically stable. We can set the function $\mu(r) = r/3$. Then, all requirements for the stochastic stability conditions are satisfied but for $LV(M) \leq 0$. To maintain stability, we require that the function $LV(M)$ be non-positive and, hence

$$LV(M) \leq 0 \Longrightarrow \frac{1}{2} \sum_i \mathcal{L}_i^2 + \sum_i m_i \mathcal{F}_i \leq 0, \ \ \forall M. \tag{29}$$

The parameter set (which includes θ_{long}, θ_{lat}, σ_{lon}, σ_{lat}, η_{lon}, and η_{lat}) is adjusted so that the stability condition of the system is maintained. Because $\sin(\cdot)$, $\cos(\cdot)$, and $\tanh(\cdot)$ are smaller than 1, then we have the following relationship:

$$\begin{aligned} \sum_i m_i \mathcal{F}_i \ \leq\ & m_1 m_4 + m_2 (m_4 - v_{i-1}) + m_3 (m_4 - v_{i-1}) \\ & + m_4 \left(a_{\mathrm{MAX}} + \eta_{\mathrm{long}} \right) + m_5 (1 + \eta_{\mathrm{lat}}) \\ & + m_6 \left(-\theta_{\mathrm{long}} m_6 \right) + m_7 \left(-\theta_{\mathrm{lat}} m_7 \right) \end{aligned}$$

$$= -\theta_{\text{long}} m_6^2 - \theta_{\text{lat}} m_7^2 + m_1 (-v_{i-1} + m_4) + m_2 m_4 + m_3 m_4 + m_4 (a_{\text{MAX}} + \eta_{\text{long}}) + m_5 (1 + \eta_{\text{lat}}) - m_2 v_{i-1} - m_3 v_{i-1}. \quad (30)$$

On the other hand,

$$\frac{1}{2} \sum_i \mathcal{L}_i^2 = \frac{1}{2} \left[\sigma_{\text{long}}^2 + \sigma_{\text{lat}}^2 \right]. \quad (31)$$

Then,

$$\begin{aligned} &\frac{1}{2} \sum_i \mathcal{L}_i^2 + \sum_i m_i \mathcal{F}_i \\ \leq\ & -\theta_{\text{long}} m_6^2 - \theta_{\text{lat}} m_7^2 + m_1 m_4 + m_2 m_4 + m_3 m_4 \\ & + m_4 (a_{\text{MAX}} + \eta_{\text{long}}) + m_5 (1 + \eta_{\text{lat}}) - m_2 v_{i-1} \\ & - m_3 v_{i-1} + \frac{1}{2} \left[\sigma_{\text{long}}^2 + \sigma_{\text{lat}}^2 \right]. \end{aligned} \quad (32)$$

The sum of the first term and the second term on the right-hand side (RHS) of Eq. (32), *i.e.*, $-\theta_{\text{long}} m_6^2 - \theta_{\text{lat}} m_7^2$, is always negative. Obviously, there exist sufficiently large positive constants: θ_{long} and θ_{lat} (they both are positive by default, so the noise fluctuates around 0), so that the RHS is negative, while this ensures that $LV\,(M)$ is negative, and a stability condition is achieved.

4. Numerical study

In this study, we use the following parameters: l_{f} and l_{r} are 1.1 m and 1.3 m, respectively; a_{MAX} and b are set to be 3.0 m/s^2 and 3.21 m/s^2, respectively. T in the IDM model is set to be 1.5 s. v_{d} is set to be 60 km/h or 16.6 m/s.

4.1. Stability analysis

We use the following state in simulation to investigate stability conditions: $[y, \psi, v, \delta, Z_{\text{long}}, Z_{\text{lat}}] = [-1.01, 1, 16.7, 1, 0.97, -0.96]$. We first investigate the stability evolution given different ψ and the δ, by examining the function $LV\,(M)$, while keeping other parameters unchanged. The condition $y = -1.01$ means that a vehicle is located on the right of the middle line of a lane. The contour plot of $LV\,(M)$ is illustrated in Fig. 7. From Fig. 7(a) to Fig. 7(d), the parameters θ_{long} and θ_{lat} keep increasing from 0.5 to 3. When the function $LV\,(M)$ is negative, the system is stable. The isogram with $LV\,(M) = 0$ can be identified from the figure. In Fig. 7(a), when ψ is about -0.3 (or approximately 17°), and the δ is about 0.25 (approximately 17° also), the system becomes unstable, as the $LV\,(M)$ tends to be positive. As concluded from Eq. (32), the increase of θ_{long} and θ_{lat} will stabilize the system, as the $LV\,(M)$ decreases. This can be observed in Figs. 7(b)–7(d), where the isogram of $LV\,(M) = 0$ tends to move down to theleft. The stable region increases with the augment of two parameters θ_{long} and θ_{lat}.

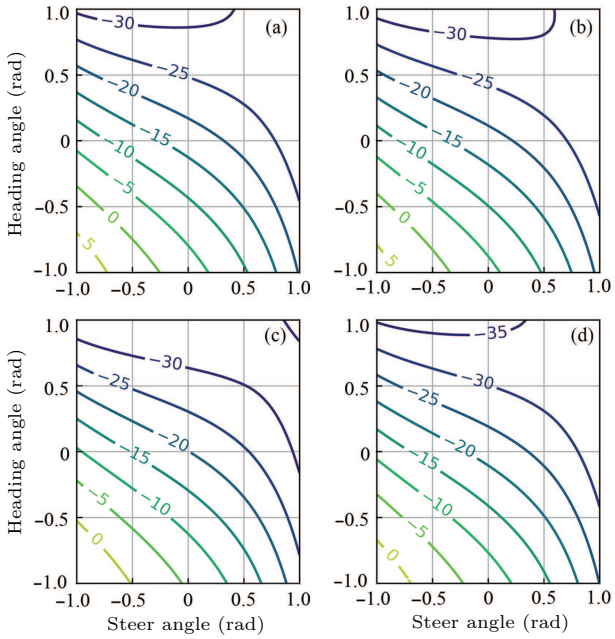


Fig. 7. *LV* function values for different parameters. (a) $\theta_{\text{long}} = 0.5$ and $\theta_{\text{lat}} = 0.5$; (b) $\theta_{\text{long}} = 1$ and $\theta_{\text{lat}} = 1$; (c) $\theta_{\text{long}} = 2$ and $\theta_{\text{lat}} = 2$; (d) $\theta_{\text{long}} = 3$ and $\theta_{\text{lat}} = 3$.

To investigate the influence of the parameters on the *LV* function, which is a direct measure of stochastic stability, we present the contour given different model parameters. The state is fixed at $[y, \psi, v, \delta, Z_{\text{long}}, Z_{\text{lat}}] = [-1.01, 1, 16.7, 1, 0.97, -0.96]$. The results are presented in Fig. 8. The influence of θ_{long} and θ_{lat} are given in Fig. 8(a) and those of σ_{long}, σ_{lat} are given in Fig. 8(b). Figure 8(a) shows that by increasing both θ_{long} and θ_{lat} the system can be stabilized, as the *LV* function value keeps decreasing. This is because greater θ means greater regression speed of the noise toward equilibrium point (0 in our case), which leads to less noise in the system. While from Fig. 8(b), it can be concluded that by increasing both noise levels (*i.e.*, increasing σ_{long} and σ_{lat}), the system will be destabilized.

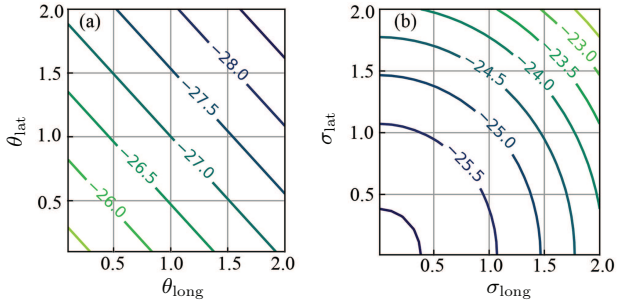


Fig. 8. *LV* function values for different model parameters.

4.2. Single vehicle acceleration from standstill

First, we place a vehicle at $x = -3$ km, and the vehicle accelerates from zero speed to free-flow speed (60 veh/h). Figure 9 shows the simulation states by using the Euler discretization scheme in Eq. (21). The time step length is 0.5 s and the simulation horizon is 600 s, or 10 min. Figure 9(a) shows

the 2D path. It can be seen that the trajectory does not exactly follow the middle line ($y = 0$), but fluctuates. Figure 9(b) displays the heading angle; figure 9(c) shows the variation of speed with time, and figure 9(d) exhibits the steering angle varying with time. The speed profile is relatively smooth, as the vehicle tries to accelerate to the speed limit. The steering angle in Fig. 9(d), on the other hand, keeps changing and fluctuating around zero. It can be concluded that the simulated vehicle driver tries to center himself within the lane. However, owing to the randomness, the heading angle fluctuates, which is consistent with the driver's intuition that will use the steering angle to relocate the vehicle in the middle of the lane.

We simulate the system paths 300 times with the same initial state for 1 min, and show 50 of the system paths in Fig. 10 (too many simulation paths will overlap and the curves cannot be distinguished). The setting in this figure is the same as that in Fig. 9. It is observed that only the acceleration in Fig. 10(c) displays little fluctuation. Other trajectories all show various fluctuations. Given a specific moment, the state obeys a certain distribution. Distributions of the lateral location (*i.e.*, y), the steering angle (δ), and heading angle (ψ) are given in Fig. 11, Figure 11(a) shows the lateral distribution at several moments. The initial state is 0 (*i.e.*, the vehicle is initially located exactly on the middle line of the lane). After about 50 s (exactly 49.04 s in the plot), the deviation in the lateral location reaches about 0.6 m ($\pm$0.3 m). The distribution of the lateral location continuously evolves toward a greater variance. The said distribution also exists for the steering angle in Fig. 11(b) and the heading angle is shown in Fig. 11(c) subplot. Figure 12 shows the comparison of the standard deviation of the marginal distribution between the simulation result and the real world dataset (NGSIM, us101 case). It can be seen that the general trend of the standard deviation follows the real-world dataset.

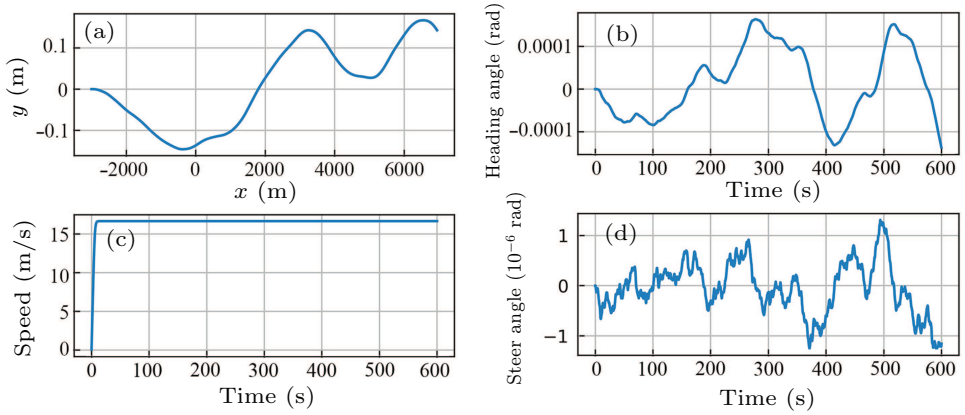


Fig. 9. States of evolution of single sample: (a): spatial trajectory, (b) heading angle, (c) longitudinal speed, and (d) steering angle.

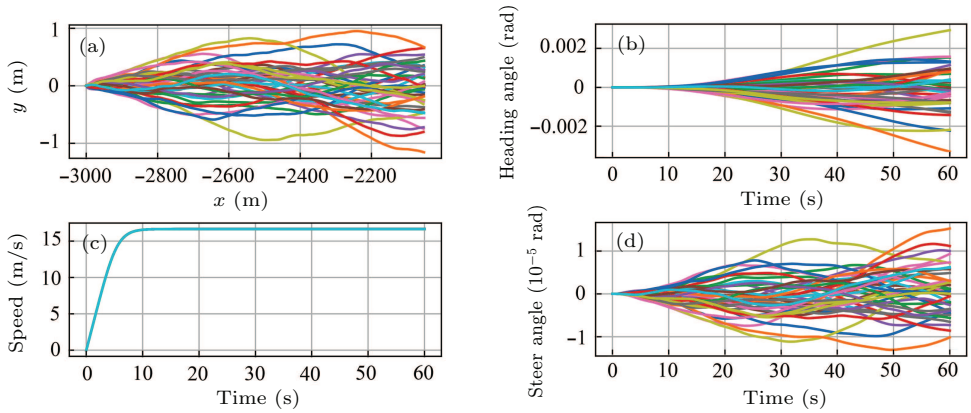


Fig. 10. States of evolution of 50 paths with the same initial state: (a) spatial trajectory, (b) heading angle, (c) longitudinal speed, and (d) steering angle.

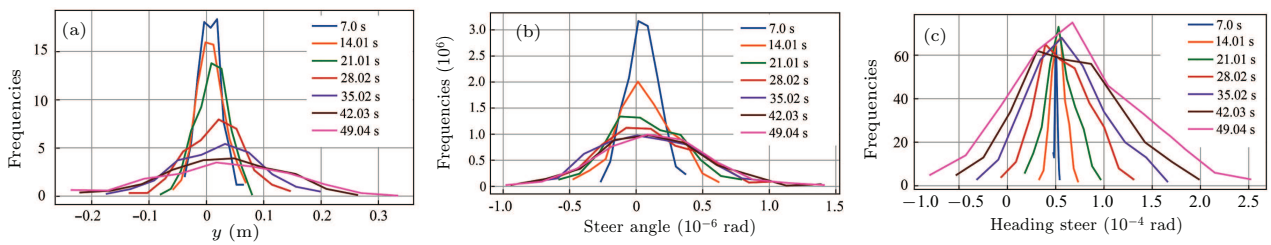


Fig. 11. Marginal distribution of model of 300 paths: (a) lateral coordinate distribution; (b) the steering angle distribution, and (c) heading angles distribution.

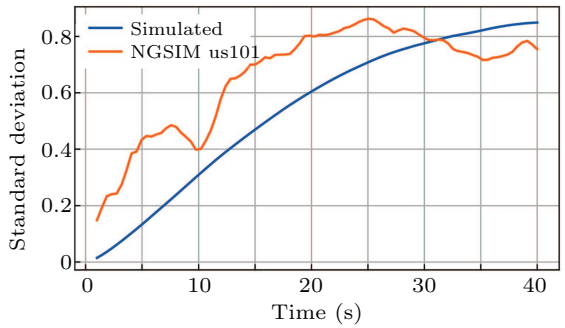


Fig. 12. (a) Standard deviation of marginal lateral distribution *versus* time and (b) frequencies *versus* heading steer at various times.

4.3. A platoon with a leading vehicle

In this example, we use a leading vehicle at a fluctuating speeds that mimic a stop-and-go traffic flow subject to a state of congestion. There are five vehicles in the platoon, including the leading vehicle, whose state is given by the model input. The speed profile of the leading vehicle is given in Fig. 13. We use a sin function to generate acceleration. and then the speed profile and longitudinal location are calculated. The vehicle accelerates from a standstill to a free-flow speed, and then stops completely. This process iterates several times.

We simulate five vehicles. The initial space headways among the five vehicles are all 30 m. The leading vehicle is located at $x = 0$ at the initial moment $t = 0$. Each vehicle accelerates from a standstill. The state evolution of the second vehicle (the vehicle just behind the leader vehicle) and the fifth vehicle are given in Figs. 14 and 15, respectively. The basic layouts of these figures are the same as the layout in Fig. 10. Although we simulate the path 300 times, each figure presents the paths of 30 simulations using the Euler scheme, as too many paths will overlap. Figure 14(a) shows the x–y trajectories. Figure 14(b) displays the heading angle evolutions. The behaviors in Figs. 14(b)–14(d) are different from the case of free driving without a leader (*i.e.*, the case in Fig. 10). Figure 14(c) shows that the speed profile is very like that of the leader vehicle in Fig. 13. When the speed is zero, the vehicle is at a standstill and the steering will not change. This is demonstrated in Fig. 14(d). For instance, during the interval from about 300 s to 400 s, the speed of the vehicle is nearly zero, and the steering angle is nearly unchanged without fluctuation (for a single line in Fig. 14(d), the steering angles almost remain unchanged during this interval, *i.e.*, from 300 s to 400 s), as it is calculated based on a pair of vehicles, both of which are standing still. As a result of the zero speed, the heading angle in Fig. 14(b) also remains unchanged during this interval. Similar results can be observed for the fifth vehicle in Fig. 15.

In Fig. 16, we arrange the trajectories of the five vehicles together. The speed profile propagation along the platoon can be observed in Fig. 16(c), where the follower vehicle's speed profile is always lagging, compared with that of the leading vehicle. The lateral positions of the five vehicles change all the time and are not aligned with the middle line of a lane, which is consistent with empirical observations.

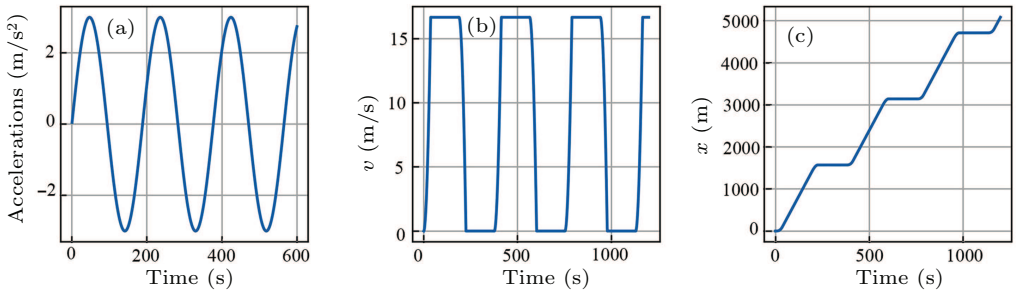


Fig. 13. Curve of acceleration, speed, and location *versus* time of leading vehicle: (a) acceleration curve, (b) speed curve, and (c) longitudinal distance.

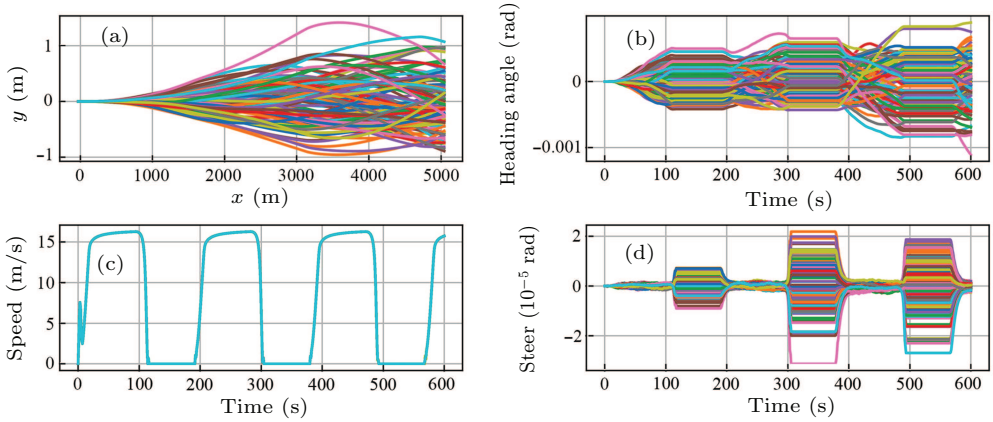


Fig. 14. State of the first vehicle in platoon: (a) spatial trajectory, (b) time-dependent heading angle, (c) time-dependent longitudinal speed, (d) time-dependent steering angle.

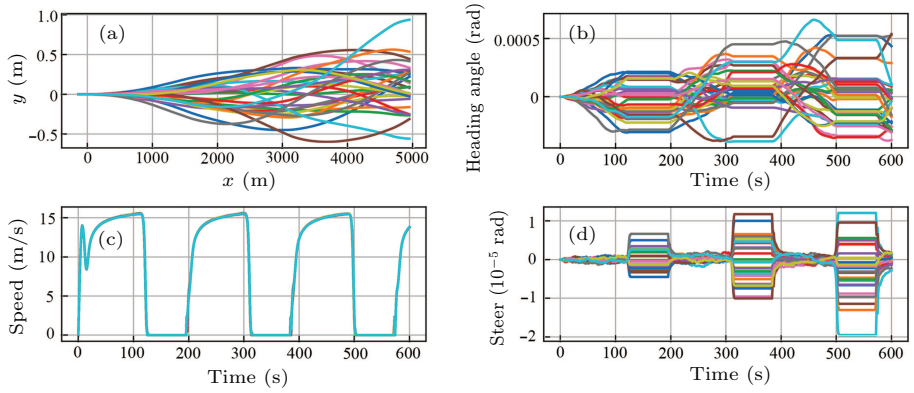


Fig. 15. State of the fifth vehicle in the platoon: (a) spatial trajectory, (b) time-dependent heading angle, (c) time-dependent longitudinal speed, and (d) time dependent steering angle.

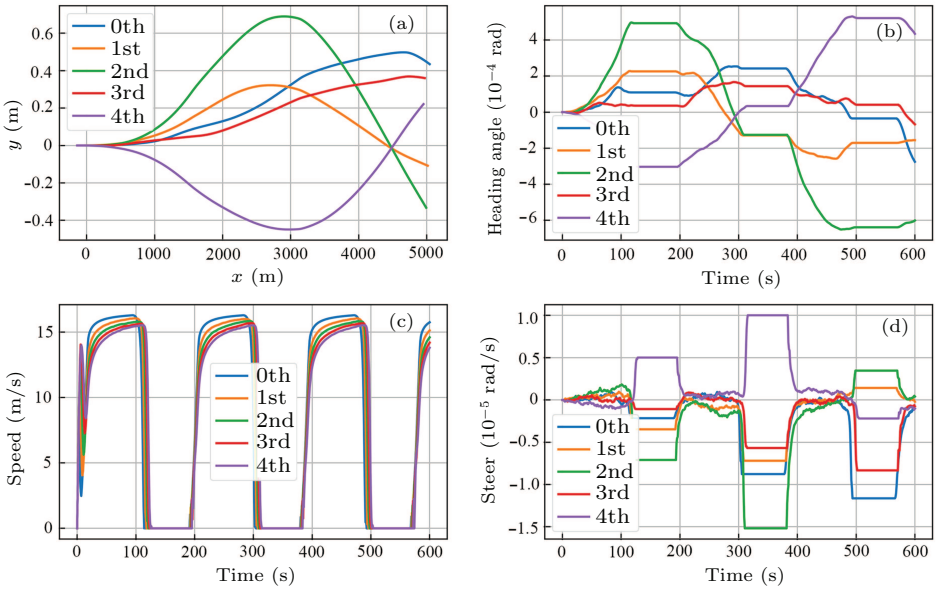


Fig. 16. Platoon dynamics evolution: (a) spatial trajectory, (b) time-dependent heading angle, (c) time-dependent longitudinal speed, and (d) time-dependent steering angle.

5. Conclusions and remarks

Vehicular modeling becomes an indispensable component for traffic flow studies in an era of connected and autonomous vehicles. Traditional models, mainly at a microscopic level, focus on drivers' reactions to leading vehicles, and neglect vehicle dynamics, or overlook 2D stochasticity. Some famous traffic flow or autonomous vehicle simulators, which are based on a driver behavior model, cannot reproduce real world characteristics. To deal with this issue, we use the merits of the famous intelligent driver model, and develop a stochastic 2D IDM model, with vehicular dynamics. Control inputs of the model include longitudinal acceleration and steering rate, with both developed based on ideas of the IDM and optimal velocity models. Both longitudinal noise and lateral noise are embedded in the model. The numerical simulations show that this model can reproduce stochastic driver-vehicle unit behavior.

This model can be extended or applied to the following ways. (i) In the era of CAV, the information comes from both a leader vehicle and road sides, which can inform the vehicle's driver of downstream traffic flow states. Hence, a more complex stimulus–reaction formulation can be derived. (ii) The proposed model can be applied to stochastic vehicular trajectory inference or predictions. Major prediction methods use deep network as a tool, but training is needed before applying it. In our model, the parameters can be adjusted and the model can predict a vehicle's dynamics in more detail. (iii) In the model, noise is constructed from the Brownian motion. Sometimes a more complex noise structure may be considered, such as the fractal Brownian motion.[4] (iv) In the proposed framework, the Rajamani vehicle model is used. As there are many levels of vehicle dynamic models, more complex ones can be employed. The resulting models may have more capabilities for describing the driver–road–vehicle–environment system.

Acknowledgements

Project supported by the National Key Research and Development Program of China (Grant No. 2021YFE0194400),

the National Natural Science Foundation of China (Grant Nos. 52272314 and 52131202), the Fund for Humanities and Social Science from the Ministry of Education of China (Grant No. 21YJCZH116), and the Public Welfare Scientific Research Project (Grant No. LGF22E080007).

References

[1] Sun Y, Ge H and Cheng R 2019 *Physica A* **534** 122377
[2] Xu L, Li Y and Feng H Z 2018 *Proceedings of the Chinese Automation Congress (CAC)*, November 3–December 2, 2018, Xian, China, p. 1146
[3] Li T, Ngoduy D, Hui F and Zhao X 2020 *Transportmetrica B: Transport Dynamics* **8** 150
[4] Wang Z, Ge H and Cheng R 2020 *Physica A* **540** 122988
[5] Navas F and Milanés V 2019 *Transportation Research Part C: Emerging Technologies* **108** 167
[6] Jiang Y, Wang S, Yao Z, Zhao B and Wang Y 2021 *Physica A* **582** 126262
[7] Liang J Y, Zhang L L, Luan X D, Guo J L, Lao S Y and Xie Y X 2017 *Acta Phys. Sin.* **66** 194501 (in Chinese)
[8] Bando M, Hasebe K, Nakayama A, Shibata A and Sugiyama Y 1995 *Phys. Rev. E* **51** 1035
[9] Ni X and Huang H 2019 *Chin. Phys. B* **28** 098901
[10] Treiber M and Kesting A 2017 *Transpation Research Procedia* **23** 174
[11] Azam M S, Bhaskar A and Haque M M 2022 *Transpmetrica A: Transp. Sci.* **18** 367
[12] Delpiano R, Herrera M J C and Coeymans A J E 2015 *Transpmetrica A: Transp. Sci.* **11** 636
[13] Sharath M N and Velaga N R 2020 *Transportation Research Part C: Emerging Technologies* **120** 102780
[14] Tian J, Zhu C, Chen D, Jiang R, Wang G and Gao Z 2021 *Transpation Research Part B: Methodological* **143** 160
[15] Gunay B 2007 *Transpation Research Part B: Methodological* **41** 722
[16] Ni D H 2015 *Traffic flow theory: Characteristics, Experimental Methods, and Numerical Techniques* (Butterworth-Heinemann: Elsevier Science)
[17] Pipes L A 1953 *J. Appl. Phys.* **24** 274
[18] Gazis D C, Herman R and Rothery R W 1961 *Operations Research* **9** 545
[19] Gipps P G 1981 *Transpation Research Part B: Methodological* **15** 105
[20] Helbing D, Hennecke A, Shvetsov V and Treiber M 2002 *Mathematical and Computer Modelling* **35** 517
[21] Liu Y J, Zhang H L and He L 2012 *Chin. Phys. Lett.* **29** 104502
[22] Delpiano R, Herrera J C, Laval J and Coeymans J E 2020 *Transpation Research Part C: Emerging Technologies* **114** 504
[23] Li Y, Zhang L, Peeta S, Pan H, Zheng T, Li Y and He X 2015 *Nonlinear Dyn.* **80** 227
[24] Peng G H 2020 *Chin. Phys. B* **29** 084501
[25] Zeng J W, Qian Y S, Wei X T and Feng X 2018 *Chin. Phys. B* **27** 124502
[26] Chen J, Chen J Y, Li M and Hu M B 2019 *Chin. Phys. B* **28** 048901
[27] Jiang R, Jin C J, Zhang H M, Huang Y X, Tian J F, Wang W, Hu M B, Wang H and Jia B 2018 *Transpation Research Part C: Emerging Technologies* **94** 83
[28] Bouadi M, Jia B, Jiang R, Li X and Gao Z Y 2022 arXiv: 2203.04877
[29] Laval J A, Toth C S and Zhou Y 2014 *Transpation Research Part B: Methodological* **70** 228
[30] Xu T and Laval J 2020 *Transpation Research Part B: Methodological* **134** 210
[31] Yuan K, Laval J, Knoop V L, Jiang R and Hoogendoorn S P 2017 *Transp. B: Transp. Dyn.* **7** 915
[32] Tomas-Gabarron J B, Egea-Lopez E and Garcia-Haro J 2013 *IEEE Trans. Intell. Transp. Syst.* **14** 1930
[33] Allen R W, Szostak H T, Klyde D H, Rosenthal T J and Owens K J 1992 *Vehicle Dynamic Stability and Rollover* (Michigan: National Highway Traffic Safety Administration)
[34] Rajamani R 2012 *Vehicle Dynamics and Control* (Boston, MA: Springer US)
[35] Makridis M, Fontaras G, Ciuffo B and Mattas K 2019 *Transp. Res. Rec.* **2673** 762
[36] Kesting A, Treiber M and Helbing D 2010 *Phil. Trans. R. Soc. A* **368** 4585
[37] Mao X R 1991 *Stability of Stochastic Differential Equations with Respect to Semimartingales* (Harlow: Longman)